Mitochondrial respiration in rats during hypothermia resulting from central drug administration

Mitochondrial respiration in rats during hypothermia resulting from central drug administration

Gianluca Sgarbi[1#] Timna Hitrec[2#] Roberto Amici[2], Alessandra Baracca[1], Alessia Di Cristoforo[2], Francesca Liuzzi[1], Marco Luppi[2], Giancarlo Solaini[1], Fabio Squarcio[2], Giovanni Zamboni[2], and Matteo Cerri[2]*

 # These authors contributed equally to this work

1 Department of Biomedical and Neuromotor Sciences (DIBINEM), Laboratory of Biochemistry and Mitochondrial Pathophysiology, University of Bologna, 40126 Bologna, Italy.

2 Department of Biomedical and Neuromotor Sciences (DIBINEM), Laboratory of Autonomic and Behavioral Physiology. University of Bologna, 40126 Bologna, Italy

*** Correspondence**:

Corresponding Author:
Matteo Cerri
matteo.cerri@unibo.it
Piazza di Porta S.Donato, 2 40126 – Bologna – Italy

Keywords: Torpor, Hypothermia, Mitochondria, Raphe Pallidus, Adenosine

Running title: Mitochondrial respiration in hypothermic rodents

Abstract

The ability to induce a hypothermia resembling that of natural torpor would be greatly beneficial in medical and non-medical fields. At present, two procedures based on central nervous pharmacological manipulation have been shown to be effective in bringing core body temperature well below 30°C in the rat, a non-hibernator: the first, based on the inhibition of a key relay in the central thermoregulatory pathway, the other, based on the activation of central adenosine A1 receptors. Although the role of mitochondria in the activation and maintenance of torpor have been extensively studied, no data are available for centrally induced hypothermia in non-hibernators. Thus, in the present work the respiration rate of mitochondria in the liver and in the kidney of rats following the aforementioned hypothermia-inducing treatments was studied. Moreover, in order to have an internal control, the same parameters were assessed in a well consolidated model, i.e. mice during fasting-induced torpor. Our results show that state 3 respiration rate, which significantly decreased in the liver of mice, was unchanged in rats. An increase of state 4 respiration rate was observed in both species, although it was not statistically significant in rats under central adenosine stimulation. Also, a significant decrease of the respiratory control ratio was detected in both species. Finally, no effects were detected in kidney mitochondria in both species. Overall, in these hypothermic conditions liver mitochondria of rats remained active and apparently ready to be re-activated to produce energy and warm up the cells. These findings can be interpreted as encouraging in view of the finalization of a translational approach to humans.

Introduction

The ability to induce a hypothermia resembling that of natural torpor would be greatly beneficial in medical and non-medical fields (Lee, 2008; Bouma *et al.*, 2012; Cerri *et al.*, 2016; Cerri, 2017; Gorr, 2017; Griko & Regan, 2018; Chouker *et al.*, 2019; Cerri *et al.*, 2021; Puspitasari *et al.*, 2021). In particular, and contrary to what observed in forced hypothermia (Vicent *et al.*,

2017), the lack of any autonomic response aimed at defending or maintaining homeothermic body temperature, as occurs in natural torpor, could lead to a safer use of therapeutic deep hypothermia.

The lack of activation of the autonomic cold defense pathway during torpor induction may be reasonably caused by the inactivation of the neural pathway that connect the hypothalamus, where the putative torpor-inducing neurons are located (Hitrec *et al.*, 2019; Hrvatin *et al.*, 2020; Takahashi *et al.*, 2020; Zhang *et al.*, 2020), with thermogenic organs. In accordance with this view, two procedures, involving a pharmacological manipulation of neural thermoregulatory circuits, have been shown to be effective in bringing core body temperature (Tb) well below 30°C in the rat, a non-hibernator: i) the inhibition of neurons within the brainstem region of the Raphe Pallidus (Cerri *et al.*, 2013), a key thermoregulatory area that controls thermoeffectors such as brown adipose tissue and cutaneous vasomotion (Zaretsky *et al.*, 2003; Cerri *et al.*, 2010; Morrison *et al.*, 2014); ii) the activation of the central Adenosine A1 receptors (A1AR) by intracerebroventricular administration of a A1AR receptor agonist (Tupone *et al.*, 2013).

The resemblance of the hypothermia induced by central drug administration to natural torpor is mostly epitomized by the hypothermic course of Tb, that is paralleled by changes concerning either brain electrical activity and heart rate or a sleep loss, recovered at the return to the euthermic Tb (Cerri *et al.*, 2013; Tupone *et al.*, 2013). However, although it has been firmly established that the Tb reduction in torpor is driven by a reduction in metabolic rate (Heldmaier *et al.*, 2004; Brown *et al.*, 2007) the physiological mechanisms and molecular signalling concerning the onset and duration of such a metabolic inactivation are still largely unknown.

The paramount oxidative character of mammalian cell metabolism mainly (Rolfe & Brown, 1997) rests on the capacity of mitochondria to completely oxidize the fuels while supplying substrates and intermediate molecules to synthesize essential compounds for the cells. In this oxidative process, reducing equivalents in the form of NADH and $FADH_2$ are transferred to oxygen through the respiratory chain complexes, allowing the transduction of the fuel chemical energy into a proton motive force ($\Delta\mu_{H+}$), that can be considered as a high energy intermediate, mainly used to drive the phosphorylation of ADP with inorganic phosphate (OXPHOS) (Van Dam *et al.*, 1980). According with a recent report (Watt *et al.*, 2010), the efficiency of this process is high being 55–60 % the values reported in current textbooks of biochemistry, although lower values, 40-41 % (Nath, 2016), or higher values up to 90% were proposed in recent theoretical considerations (Wikstrom & Springett, 2020) .The calculation was based on a H^+/ATP ratio of 3.7 and that 10 or 6 protons are moved from the matrix to the mitochondrial intermembrane space when two electrons are transferred by the respiratory chain from NADH or $FADH_2$, respectively, to molecular oxygen. However, the residual energy released by substrate oxidation, apparently lost and dissipated as heat, is important for homeotherms to maintain a constant Tb. Indeed, anatomical regions of the body where OXPHOS occurs to low levels are associated with the presence of brown adipose tissue (BAT) in which the phosphorylation of ADP hardly takes place due to the presence of mitochondrial uncoupling protein, UCP1, that dissipates energy to release heat (Klingenberg & Winkler, 1985).

Mitochondrial respiration has been described for both seasonal hibernators and mammals performing daily torpor (Brown *et al.*, 2007; Staples & Brown, 2008; Kutschke *et al.*, 2013; Grimpo *et al.*, 2014; Staples, 2014; Heim *et al.*, 2017) . Indeed, in the liver, a main contributor to rodent metabolism, mitochondrial function was reported to change during torpor/hibernation by many authors (Pehowich & Wang, 1984; Fedotcheva *et al.*, 1985; Gehnrich & Aprille, 1988; Martin *et al.*, 1999; Barger *et al.*, 2003; Muleme *et al.*, 2006; Brown & Staples, 2010; Kutschke *et al.*, 2013). In particular, in hibernating Siberian Hamsters, the State 3 respiration rate of isolated liver mitochondria was found significantly reduced, without changes in State 4 respiration. However, the depression of mitochondrial respiration during daily torpor seems to be a liver-specific mechanism as suggested by studies also performed in the kidney, the skeletal muscle and the heart of Djungarian hamster (Kutschke *et al.*, 2013)

Although the effects of hypothermia on mitochondrial metabolism has been already studied in non-hibernators at the organ level (Leducq *et al.*, 1998) and in *in vitro* models (Hendriks *et al.*, 2017), , to the best of our knowledge no measures have been carried out in a whole animal after a centrally-induced hypothermia. Considering the translational potential of such artificial conditions, we resolved to test mitochondrial respiration in rats, a non-hibernating species, following the central pharmacological induction of hypothermia. We hypothesized that mitochondria, being the main energy producer of the cells, respond to the hypothermic state in a tissue-specific manner consistent with the distinct metabolic demands and physiological roles of the tissues they belong to. On these bases, we set the following experiments to evaluate the mitochondrial function in two different organs (liver and kidney). We assayed the oxygen consumption rates by the respiratory chain under both non-phosphorylating and phosphorylating conditions, the latter in the presence of saturating ADP concentration (Barbato *et al.*, 2015) . In order to have an internal control for comparing the degree of the possible hypothermia-induced effects, the same parameters were also assessed in mice using the well consolidated model of fasting-induced torpor.

\Material and Methods

All experiments were carried out after approval by the National Health Authority (decree: No.112/2018 - PR), in accordance with the DL 26/2014 and the European Union Directive 2010/63/EU, and under the supervision of the Central Veterinary Service of the University of Bologna. All efforts were made to minimize the number of animals used and their pain and distress.

Experiments were performed on 16 C57BL/6J female mice (13-15 week old; The Jackson Laboratory, stock number 000664 | Black 6; 17-24g) and 19 male Sprague-Dawley rats (Charles River; 250-300g). Animals were housed for one week at standard animal house conditions: light-dark cycle (LD cycle) 12h:12h (L 09:00-21:00), ad libitum access to food (4RF21 diet, Mucedola, Settimo Milanese, Italy) and water, 25 ± 1°C ambient temperature (Ta), and 150 lux light intensity.

After this period, ambient conditions were changed for mice only for the subsequent three weeks in order to induce torpor during the normal daily time of activity of the experimenters. In particular the L period of the 12h:12h LD cycle was shifted to 15:00-03:00, and Ta was raised to 28 ± 1°C.

Drugs

The $GABA_A$ agonist muscimol (CAS Number 2763-96-4) was obtained by Tocris (Bristol, UK); the A1AR receptor agonist N_6-cyclohexyladenosine (CHA, CAS Number 36396-99-3) was obtained by Sigma Aldrich (St. Louis, MO). All drugs were dissolved into a vehicle solution composed of artificial cerebrospinal fluid (NaCl 125mM, KCl 3mM, $CaCl_2$ 2.5 mM, $MgSO_4$ 1.3 mM, NaH_2PO_4 1.25 mM, $NaHCO_3$ 26mM, Glucose 13 mM, pH 7.4) obtained by EcoCyte Bioscience (Austin, TX).

Surgery

Surgery was carried out in rats housed for at least one week at normal laboratory conditions. Rats were pre-anaesthetized with Diazepam (Valium, Roche, 5 mg/Kg intramuscular) and anaesthetized with Imalgene 1000 (Ketamine-HCl, Merial, 100 mg/Kg intraperitoneally). After confirming the surgical plane of anaesthesia by the absence of blink and toe-pinch reflexes, using a small animal shaver, the cranial surface was shaved, and the exposed skin was disinfected with iodine solution. Afterwards, the animal was positioned on a stereotaxic frame (Kopf instruments), the skin was incised, the periosteum was removed, and the skull surface was cleaned, making the cranial sutures clearly visible. Using a 0.5 mm drill tip, six craniotomies were made: two on the left and right frontal bones (in antero-lateral position) and two on the left and right parietal bones (in postero-lateral position) to implant four stainless steel screws to provide stability to the implant; one was positioned above the right anterior hypothalamus to insert the calibrated thermistor to record hypothalamic temperature (Thy). The final craniotomy was positioned according to the target of each experimental group.

In groups with Raphe Pallidus targeting (Muscimol and artificial cerebrospinal fluid - ACSF) (see Experimental plan, n=9), a microinjection guide cannula (C315G-SPC; Plastics One; internal cannula extension below guide: +3.5 mm) was stereotactically implanted at coordinates aiming at the RPa (-3.4 AP, 0.0 LL, -9.5 DV; (Paxinos & Watson, 2007). To assess the correct positioning of the guide cannula, a functional intraoperative test was carried out by doing a test-injection of the selective $GABA_A$ agonist muscimol (100nl, 1mM) and monitoring the effect induced on the tail temperature measured by an infrared thermocamera (Thermovision A20, Flir Systems). It is well known that the inhibition of RPa neurons causes massive cutaneous vasodilation (Blessing & Nalivaiko, 2001; Cerri *et al.*, 2010).

In group with intracerebroventricular drug administration (N_6-cyclohexyladenosine - CHA and ACSF) (see Experimental plan, n=10), a microinjection guide cannula (C315G-SPC; Plastics One; internal cannula extension below guide: +1 mm) was stereotactically implanted to aim at the left lateral ventricle (-1.2 AP, 1.3 LL, -4 DV, (Paxinos & Watson, 2007) . The location of the cannula was considered correct when progressive cerebrospinal fluid withdrawal was observed. The implant was then fixed with dental resin (ResPal, Salmoiraghi Produzione Dentaria), covering the entire surgical field, incorporating the thermistor and the screws.

After the surgery, rats were then administered with wide-spectrum antibiotics (1 µl/g Ampicilline 500mg/5ml; 0.2 µl/g di Amikacin 500mg/10ml) to prevent any infections, with 5 ml subcutaneous saline solution to prevent dehydration, and with an analgesic treatment (Rimadyl - Carprofen 5mg/ml, Pfizer – 5mg/kg). The animal's pain, distress or suffering symptoms were constantly evaluated using the Humane End Point criteria. Animals that displayed some degree of suffering symptoms were administered, as needed, with 5mg/kg of Rimadyl (Carprofen 5mg/ml, Pfizer).

Experimental plan

Overall, animals were divided in six experimental groups, four groups of rats and two of mice. The experimental plan is graphically detailed in Fig. 1.

A) RAT Muscimol:

i) Muscimol (n=4 rats): After a 7-day recovery from surgery, starting at L onset, animals were injected with the $GABA_A$ agonist muscimol (1 mM) into the Raphe Pallidus (RPa). Each animal received a total of five injections (1/h). All animals entered a hypothermic state shortly after the first injection.

ii) ACSF-RPa (n=5 rats): Animals were exposed to the same procedures for Muscimol but RPa-injected only with artificial cerebrospinal fluid (ACSF).

B) RAT CHA:

i) CHA (n=5 rats): After a 7-day recovery from surgery, at L onset, animals were injected intracerebroventricularly (icv) over the time of 2 min, with 5 µl of the A1AR agonist N_6-cyclohexyladenosine (CHA) (1mM). All animals entered a hypothermic state shortly after the injection.

ii) ACSF-icv (n=5 rats): Animals were exposed to the same procedures for group CHA but icv-injected only with ACSF.

C) MOUSE

i) Torpor (n=8 mice). Mice were induced into torpor by using the procedure described by Oelkrug, Heldmaier and Meyer, 2011. Briefly, after 3 weeks of adaptation to Ta = 28°C, with food and water ad libitum, mice were fasted for 36 hours and then exposed, at 09:00 (i.e. six hours after dark onset), to Ta = 15°C. Torpor was successfully induced within 60 min from the exposure.

ii) Control (n=8 mice). Mice were subjected to the same protocol described for group Torpor but not fasted. No sign of torpor was observed in this experimental group.

Experimental setting and temperature recording

Following one week of recovery after surgery, rats were moved in a cage hosted in a thermoregulated, ventilated, sound-attenuated box, consisting in a modified refrigerator. Two days before the experiment the hypothalamic thermistor was then wired, through a rotating swivel, to the amplifier. The signal was amplified (mod. Grass 7P511L, Astro-Med Inc, West Warwick (RI), USA), filtered (0,5 Hz high-pass), analog to digital converted (12 bit, CED Micro MK 1401 II), acquired (50Hz sampling rate), and digitally stored.

All microinjections were performed according to what described in Cerri *et al.*, 2013. Briefly, A 1m Teflon tube, with constant diameter (D.I.0.2mm, FEP-Tubing 4001005 10X1m Microbiotech/se AB, Stockholm, Sweden) was tightly connected from one side to a Hamilton 5 µl syringe (Hamilton Company, Bonaduz, Switzerland) and on the other side to the injection cannula. The syringe was placed on a microinjection pump (Harvard Apparatus), with an infusion rate set at 0.3 µl/min. The tube and the cannula were filled with the solution containing either a drug (muscimol or CHA) or ACSF, whilst the syringe was filled with colored mineral oil. The oil-drug interface, observed on a ruler, under a stereo-microscope, allowed the operator to visually control the injected volume. After the injection, the internal cannula was left in place for about 10 minutes and then was gently removed. To minimize the interaction with the animal, the pump, the syringe and the operator were located outside the experimental box, so that the animals were completely unaware to be injected.

Thirty-six hours before torpor induction, mice were moved in a two compartment-cage, consisting of a 40-cm high plexiglass cylinder divided in two semicircles by a removable plexiglass panel. This allowed to house mice in couples, each in one semicircle, impeding their interaction. The cage was hosted in a thermoregulated, ventilated, sound-attenuated box, consisting in a modified refrigerator at Ta = 28°C and moved, on the experimental day, a in a second thermoregulated, ventilated, sound-attenuated box at Ta = 15°C.

In mice, surface Tb was measured by using an infrared thermocamera (Thermovision A20, Flir Systems) positioned above the cage. Temperature was then obtained by analyzing the recorded video using a dedicated software (Thermocam research, FLIR). The highest temperature within each frame, corresponding to that of the head, was used as an index of Tb.

Tissue sampling

After four hours from the onset of either natural torpor or the hypothermic state induced by drug administration, animals were euthanized with a lethal dose of anaesthetics (Imalgene 1000, Ketamine-HCl, Merial, 100 mg/Kg intraperitoneally), and the liver and kidneys were collected. Anaesthesia has been shown not to influence the mitochondrial activity in rodents (Takaki *et al.*, 1997). Control groups were time matched. All the organs were stored in a phosphate buffered solution and immediately processed.

Mitochondria Isolation and Function

Liver and kidney mitochondria were isolated from rats and mice according to Barogi et al., 1995. Briefly, tissue was homogenized with a Potter-Elvehjem grinding chambers and pestles in buffer solution (0.22 M Mannitol, 0.07 M Sucrose, 0.1 mM EGTA, 1 mM EDTA and 20 mM HEPES, pH 7.4, containing 0.4% albumin) and then centrifuged at 2000 rpm for 10 min. in a SS34 Sorvall rotor to remove nuclei and plasma membrane fragments. The supernatants were filtered through a gauze and the eluted fractions were then centrifuged at 8000 rpm for 10 min. The pellets obtained were washed once in the above buffer devoid of albumin. Finally, mitochondria were resuspended in the buffer containing 0.25 M Sucrose, 20 mM HEPES, 0.1 mM EGTA, and 1 mM EDTA, pH 7.4, and promptly assayed to collect the main respiration parameters. Mitochondrial protein determination was performed by the biuret method (Gornall *et al.*, 1949) as previously reported (Solaini *et al.*, 1997).

Oxygen consumption rates were measured at 37°C using a Clark-type oxygen electrode as previously reported by (Barbato *et al.*, 2015). Under state 3 conditions the NADH dependent-oxygen consumption was measured by adding to mitochondria (0.1 mg) 10 mM glutamate/10 mM malate (plus 1.8 mM malonate) and

0.5 mM ADP as substrates (Bosetti *et al.*, 2004). The state 4 respiration rates were measured following the ADP consumption, and confirmed by adding the ATP synthase inhibitor oligomycin (Solaini *et al.*, 2008). We calculated the initial rate of respiration under both State 3 and State 4 conditions by evaluating the oxygen concentration decline during the first two min reaction of each state. The energetic coupling between the respiratory chain activity and the ATP synthase activity was estimated by the respiratory control ratio (RCR), namely the State 3 (phosphorylating condition) to State 4 (non-phosphorylating condition) respiration rates ratio.

Statistical analysis

The results for either hypothalamic or cutaneous temperature and those for State 3 and State 4 mitochondrial respiration, and the respiratory control ratio (RCR State 3/State 4 respiration rate), were statistically analyzed by comparing the treated animals (torpid mice and hypothermic rats) vs. the control groups (euthermic animals) by means of a Student's t-test. Statistical significance was set at $p<0.05$.

Results

The time course of rat deep brain temperature after the induction of the hypothermic state by either muscimol (Fig. 2 panel A) or CHA (Fig. 2 panel B) administration and mice cutaneous temperature after natural torpor onset (panel C) are shown. According to earlier observations (Cerri *et al.*, 2013; Tupone *et al.*, 2013; Hitrec *et al.*, 2019), a large and significant decrease in both brain and body temperature was observed in each of the three experimental conditions. Indeed, a similar decrease (about 8°C) was detected in both rat deep brain and mouse cutaneous temperature following CHA administration or natural torpor onset, respectively. At variance, in rats the temperature decrease following the induction of the hypothermic state by muscimol was much larger (about 16°C) compared to those observed under the above experimental conditions. Thy at hypothermic nadir was significantly lower in rats after muscimol than after CHA administration (21.2 ± 0.5°C and 27.6 ± 0.7 °C, respectively, $p<0.01$)

Effects of the drug-induced hypothermic state and natural torpor on liver mitochondria

Figure 3 shows the oxygen-electrode recordings of rat and mouse liver mitochondria respiring in the presence of malate/glutamate as substrates, to assay the oxidation rate of NAD^+-dependent substrates. The oxygen consumption rate of liver mitochondria isolated from rats treated with either muscimol or CHA did not show differences under State 3 (ADP-stimulated) respiratory conditions compared to the respective controls, ACSF, but it appeared to be increased under State 4 conditions (Fig. 3A and B). Incidentally, the control traces are similar to those previously reported (Rolfe and Brown, 1997), using the same isolation techniques to prepare mitochondria. The average State 3 respiration rate of rat liver mitochondria was similar with either treatment (Fig. 4A and 4B). At variance, State 4 respiration rates in rats treated with muscimol (Fig. 4A) or CHA (Fig. 4B) was higher (+29 % and +84 %, respectively) compared to ACSF treated rats (controls), however the CHA treatment only caused a statistically significant increase ($p<0.05$ *vs.* control). Consequently, the respiratory control ratio (RCR) was significantly lower in mitochondria of drug treated rats compared to controls (ACSF treated rats), ranging from -23 % in muscimol-treated rats to -41% in CHA-treated rats ($p<0.05$ and $p<0.01$ *vs.* control, respectively).

Consistently, in liver mitochondria isolated from mice, significant and opposite changes in State 3 and State 4 respiratory conditions were observed during torpor compared to control conditions (Fig 3C and 4C). Indeed, in torpid mice a 33% decrease and 40% increase of the state 3 and state 4 respiration rates, respectively were observed ($p<0.01$ and $p<0.05$ *vs.* control, respectively). Accordingly, the RCR was significantly lower (-53 %; $p<0.01$ *vs.* control) in torpid mice compared to controls (Fig. 4C).

Effects of the drug-induced hypothermic state and natural torpor on kidney mitochondria

The same polarographic analyses were also performed in mitochondria isolated from kidney and assayed as in liver (Fig. 5). Kidney mitochondria isolated from rats treated with either muscimol or CHA did

not show statistically significant changes under either State 3 or State 4 respiratory conditions compared to ACSF controls (Fig. 5 and 6). Consequently, the RCRs resulted similar in treated and control rats whatever treatment (Fig. 6A and B). Unlike the liver, kidney mitochondria isolated from torpid mice did not show statistically significant changes of respiratory parameters compared to controls (Fig. 5C and 6C).

Discussion

In the present study we examined the activity of mitochondria isolated from the liver and kidney of rats induced in hypothermia by central nervous drug administration and, in order to have an internal control for comparing the degree of the possible hypothermia-induced effects, in mice induced in natural torpor by fasting. The experiments we set to induce hypothermia in rats were based on two different methods: i) the first, highly selective, by inhibiting neurons within the Raphe Pallidus (RPa), a key brainstem structure involved in thermoregulation that drives many thermogenic effectors (Cerri *et al.*, 2013). ii) the second, by the intracerebroventricular injection of the A1AR receptor agonist CHA, (Tupone *et al.*, 2013). Both models were shown to cause a sharp decrease of the rat Tb well below 30°C, however there is no evidence in the literature whether this effect is associated with changes in mitochondrial activity, similarly to what it occurs in natural hibernators.

In both species, notable changes were observed in the liver, while no significant effect was found in the kidney. Notably, the liver State 4 respiration activity was significantly increased in both mice and rats, although, in the latter, only when CHA was administered. In the liver of mice only, this occurred together with a significant decrease in State 3 respiration. As a consequence, the RCR decreased in both species, but only in mice liver this was due to the concurrent decrease in state 3 and increase in state 4; in rats, the RCR decrease was apparently caused by the only state 4 increase.

The assay of the mitochondrial respiration is a mirror of the substrate oxidative pathways, that could be affected by alteration of substrate transporters, citric acid cycle flow, and mitochondrial electron transport chain complexes. In particular, State 3 respiration could be markedly affected by the rate of ADP phosphorylation, therefore by the activity of the adenine nucleotide transporter, the phosphate transporter, and the ATP synthase. At variance, the main parameter affecting the State 4 respiration rate is the proton leakage of the inner mitochondrial membrane (Bosetti *et al.*, 2004; Brown & Staples, 2010).

Mitochondria are responsible of about 90% of the cellular ATP production that mainly occurs through oxidative phosphorylation, a process relying on the reduction of molecular oxygen. Therefore, a decreased metabolic rate might be reasonably promoted by a decrease of the mitochondrial respiration rate (Rolfe & Brown, 1997), possibly by a specific inhibition related with torpor. A reduction in metabolic activity of the liver could induce a significant decline in energy expenditure in the mouse, since in this species the organ accounts for 17% of the oxygen consumption of the whole organism (Martin & Fuhrman, 1955). Interestingly, the mouse liver shows a specific metabolic rate that is 1.6 times higher than that observed in the corresponding organ of the rat (Wang *et al.*, 2012).

The decrease of State 3 respiration rate observed in mice liver mitochondria is consistent with data previously reported in the literature (Brown & Staples, 2010). Indeed, State 3 respiration reduction was also reported in other hibernating species, including the squirrel (Gehnrich & Aprille, 1988; Martin *et al.*, 1999; Barger *et al.*, 2003), the dwarf Siberian hamster (Brown *et al.*, 2007), and the Djungarian hamster (Kutschke *et al.*, 2013). The latter study highlighted both the specificity of decreased State 3 respiration in liver and its degree, that correlated with the decrease of body temperature. On the contrary, no decrease in state 3 was observed in the rats used in these experiments, while state 4 was increased (although not significantly in the RPa group).

This effect was not observed in previous studies: no change of State 4 was reported in mice (Brown & Staples, 2010), nor in ground squirrel (Martin *et al.*, 1999), nor in the dwarf Siberian hamster (Brown *et al.*, 2007), whereas a reduction was observed in the arctic ground squirrel (Barger *et al.*, 2003) and in the Djungarian hamster (Kutschke *et al.*, 2013). The State 4 respiration enhancement in the liver of both species examined deserves interest. The causes for this can only be speculated, suggesting, for instance, a temperature-dependent effect on the fluidity of the mitochondrial membranes (Baracca *et al.*, 1994). Whether this may have any functional significance is hard to tell. Indeed, the increased respiration rate is due to dissipation of the proton gradient through the inner mitochondrial membrane, allowing generation of heat from the energy released by the respiratory chain. However, at a low Tb, such effect might be negligible.

Overall, from a comparative point of view, the lack of reduction of State 3 in liver mitochondria in the hypothermic rat, suggests that the reduced State 3 respiration rate in the liver of mice is not merely caused by the decrease in Tb, but it is rather a specific feature of torpor and hibernation. The torpor specific changes of liver mitochondrial activity could be useful to investigate if a molecular fingerprint of torpor exists at cellular level**.** Their identification could lead to the pinpointing of specific markers of torpor that could help to distinguish torpor-specific organs from those only responding to the decrease in temperature. On the contrary, the similar State 4 respiration change observed in both species might suggest that it is the consequence of hypothermia rather than a torpor-specific mitochondrial activity modulation.

If, on one hand, the data from the liver suggest that the hypothermia induced by central nervous drug administration and that occurring in natural torpor have some intrinsic differences in mitochondrial functions, in the kidney the results do not point to the same direction. In fact, kidney mitochondrial activity does not seem influenced in both mice and rats. This is in accordance to what already observed in the Djungarian hamster (Kutschke *et al.*, 2013), in which the lack of State 3 decrease was seen as an evidence indicating that the mitochondrial activity was maintained. In clinical practice, kidneys are particularly at risk of suffering of ischemia-reperfusion injury, due to their high metabolism and oxygen consumption, and are rich in mitochondria. It is still debated whether therapeutic hypothermia and the subsequent rewarming can efficiently limit the damage induced by the hypoxic/ischemic state in kidneys (Susantitaphong *et al.*, 2012; De Rosa *et al.*, 2017). Conversely, hibernating mammals are able to drastically lower their metabolic rate and Tb without any reported pathological outcome in the kidneys. Hibernation has shown to preserve renal tubular cells, the number of mitochondria, and their structure (Hendriks et al., 2017). The understanding of the molecular mechanisms underlying such efficient organ preservation, while enduring extreme physiological conditions, could bring many useful outcomes, such as developing new protocols for preserving kidneys from ischemia/reperfusion injury during transplants.

In conclusion, these data could be interpreted as encouraging in view of the finalization of a translational approach to a so-called "synthetic" torpor condition in humans for medical (Cerri, 2017; Luppi *et al.*, 2019; Hitrec *et al.*, 2021) and space (Cerri *et al.*, 2016; Griko & Regan, 2018; Tinganelli *et al.*, 2019; Cerri *et al.*, 2021) applications. Mitochondrial activity is not apparently specifically compromised in rats kept in a hypothermic condition and may promptly be re-activated to warm up the liver cells even from very low levels of Tb. This is especially relevant since the liver will have to support the arousal by providing the organism with the adequate substrates and therefore will have to count on an effective mitochondrial function.

Conflict of Interest *The authors declare that the research was conducted in the absence of any commercial or financial relationships that could be construed as a potential conflict of interest*.

Author Contributions:

Timna Hitrec and Gianluca Sgarbi share first authorship of this publication.

Experiment ideation: Roberto Amici, Matteo Cerri, Giovanni Zamboni,
Experimental plan design: Roberto Amici, Alessandra Baracca, Matteo Cerri, Timna Hitrec, Gianluca Sgarbi, Giancarlo Solaini, Giovanni Zamboni.
Surgery: Alessia Di Cristoforo, Timna Hitrec

Microinjection in rats: Alessia Di Cristoforo, Timna Hitrec, Fabio Squarcio
Fasting-induced torpor in mice: Alessia Di Cristoforo, Timna Hitrec, Fabio Squarcio
Sample collection: Matteo Cerri, Timna Hitrec , Marco Luppi,
Measurement of mitochondrial function: Francesca Liuzzi, Gianluca Sgarbi
Mitochondrial data analysis: Gianluca Sgarbi
Temperature data analysis: Timna Hitrec
Analysis of the results: Roberto Amici, Alessandra Baracca, Matteo Cerri, Alessia Di Cristoforo, Timna Hitrec, Francesca Liuzzi, Marco Luppi, Gianluca Sgarbi, Giancalro Solaini, Fabio Squarcio, Giovanni
Interpretation of the findings: Roberto Amici, Alessandra Baracca, Matteo Cerri, Timna Hitrec, Gianluca Sgarbi, Giancarlo Solaini
Manuscript writing: Roberto Amici, Alessandra Baracca, Matteo Cerri, Timna Hitrec, Gianluca Sgarbi, Giancarlo Solaini
Manuscript editing: Roberto Amici, Alessandra Baracca, Matteo Cerri, Timna Hitrec, Gianluca Sgarbi, Giancarlo Solaini, Giovanni Zamboni

Funding
The experiments were funded by the project FARB - Warm up to wake up – from the University of Bologna

References

Baracca, A., Barzanti, V., Lenaz, G. & Solaini, G. (1994) Dietary lipids and 5'-nucleotidase activity of rat cell plasma membranes. *Biochem Biophys Res Commun*, **199**, 99-105.

Barbato, S., Sgarbi, G., Gorini, G., Baracca, A. & Solaini, G. (2015) The inhibitor protein (IF1) of the F1F0-ATPase modulates human osteosarcoma cell bioenergetics. *J Biol Chem*, **290**, 6338-6348.

Barger, J.L., Brand, M.D., Barnes, B.M. & Boyer, B.B. (2003) Tissue-specific depression of mitochondrial proton leak and substrate oxidation in hibernating arctic ground squirrels. *Am J Physiol Regul Integr Comp Physiol*, **284**, R1306-1313.

Barogi, S., Baracca, A., Parenti Castelli, G., Bovina, C., Formiggini, G., Marchetti, M., Solaini, G. & Lenaz, G. (1995) Lack of major changes in ATPase activity in mitochondria from liver, heart, and skeletal muscle of rats upon ageing. *Mech Ageing Dev*, **84**, 139-150.

Blessing, W.W. & Nalivaiko, E. (2001) Raphe magnus/pallidus neurons regulate tail but not mesenteric arterial blood flow in rats. *Neuroscience*, **105**, 923-929.

Bosetti, F., Baracca, A., Lenaz, G. & Solaini, G. (2004) Increased state 4 mitochondrial respiration and swelling in early post-ischemic reperfusion of rat heart. *FEBS Lett*, **563**, 161-164.

Bouma, H.R., Verhaag, E.M., Otis, J.P., Heldmaier, G., Swoap, S.J., Strijkstra, A.M., Henning, R.H. & Carey, H.V. (2012) Induction of torpor: mimicking natural metabolic suppression for biomedical applications. *J Cell Physiol*, **227**, 1285-1290.

Brown, J.C., Gerson, A.R. & Staples, J.F. (2007) Mitochondrial metabolism during daily torpor in the dwarf Siberian hamster: role of active regulated changes and passive thermal effects. *Am J Physiol Regul Integr Comp Physiol*, **293**, R1833-1845.

Brown, J.C. & Staples, J.F. (2010) Mitochondrial metabolism during fasting-induced daily torpor in mice. *Biochim Biophys Acta*, **1797**, 476-486.

Cerri, M. (2017) *The Central Control of Energy Expenditure: Exploiting Torpor for Medical Applications*.

Cerri, M., Hitrec, T., Luppi, M. & Amici, R. (2021) Be cool to be far: Exploiting hibernation for space exploration. *Neurosci Biobehav Rev*, **128**, 218-232.

Cerri, M., Mastrotto, M., Tupone, D., Martelli, D., Luppi, M., Perez, E., Zamboni, G. & Amici, R. (2013) The inhibition of neurons in the central nervous pathways for thermoregulatory cold defense induces a suspended animation state in the rat. *J Neurosci*, **33**, 2984-2993.

Cerri, M., Tinganelli, W., Negrini, M., Helm, A., Scifoni, E., Tommasino, F., Sioli, M., Zoccoli, A. & Durante, M. (2016) Hibernation for space travel: Impact on radioprotection. *Life Sciences in Space Research*, **11**, 1-9.

Cerri, M., Zamboni, G., Tupone, D., Dentico, D., Luppi, M., Martelli, D., Perez, E. & Amici, R. (2010) Cutaneous vasodilation elicited by disinhibition of the caudal portion of the rostral ventromedial medulla of the free-behaving rat. *Neuroscience*, **165**, 984-995.

Chouker, A., Bereiter-Hahn, J., Singer, D. & Heldmaier, G. (2019) Hibernating astronauts-science or fiction? *Pflugers Arch*, **471**, 819-828.

De Rosa, S., Antonelli, M. & Ronco, C. (2017) Hypothermia and kidney: a focus on ischaemia-reperfusion injury. *Nephrol Dial Transplant*, **32**, 241-247.

Fedotcheva, N.J., Sharyshev, A.A., Mironova, G.D. & Kondrashova, M.N. (1985) Inhibition of succinate oxidation and K+ transport in mitochondria during hibernation. *Comp Biochem Physiol B*, **82**, 191-195.

Gehnrich, S.C. & Aprille, J.R. (1988) Hepatic gluconeogenesis and mitochondrial function during hibernation. *Comp Biochem Physiol B*, **91**, 11-16.

Gornall, A.G., Bardawill, C.J. & David, M.M. (1949) Determination of serum proteins by means of the biuret reaction. *J Biol Chem*, **177**, 751-766.

Gorr, T.A. (2017) Hypometabolism as the ultimate defence in stress response: how the comparative approach helps understanding of medically relevant questions. *Acta Physiol (Oxf)*, **219**, 409-440.

Griko, Y. & Regan, M.D. (2018) Synthetic torpor: A method for safely and practically transporting experimental animals aboard spaceflight missions to deep space. *Life Sci Space Res (Amst)*, **16**, 101-107.

Grimpo, K., Kutschke, M., Kastl, A., Meyer, C.W., Heldmaier, G., Exner, C. & Jastroch, M. (2014) Metabolic depression during warm torpor in the Golden spiny mouse (Acomys russatus) does not affect mitochondrial respiration and hydrogen peroxide release. *Comp Biochem Physiol A Mol Integr Physiol*, **167**, 7-14.

Heim, A.B., Chung, D., Florant, G.L. & Chicco, A.J. (2017) Tissue-specific seasonal changes in mitochondrial function of a mammalian hibernator. *Am J Physiol Regul Integr Comp Physiol*, **313**, R180-R190.

Heldmaier, G., Ortmann, S. & Elvert, R. (2004) Natural hypometabolism during hibernation and daily torpor in mammals. *Respir Physiol Neurobiol*, **141**, 317-329.

Hendriks, K.D.W., Lupi, E., Hardenberg, M.C., Hoogstra-Berends, F., Deelman, L.E. & Henning, R.H. (2017) Differences in mitochondrial function and morphology during cooling and rewarming between hibernator and non-hibernator derived kidney epithelial cells. *Sci Rep*, **7**, 15482.

Hitrec, T., Luppi, M., Bastianini, S., Squarcio, F., Berteotti, C., Lo Martire, V., Martelli, D., Occhinegro, A., Tupone, D., Zoccoli, G., Amici, R. & Cerri, M. (2019) Neural control of fasting-induced torpor in mice. *Sci Rep*, **9**, 15462.

Hitrec, T., Squarcio, F., Cerri, M., Martelli, D., Occhinegro, A., Piscitiello, E., Tupone, D., Amici, R. & Luppi, M. (2021) Reversible Tau Phosphorylation Induced by Synthetic Torpor in the Spinal Cord of the Rat. *Front Neuroanat*, **15**, 592288.

Hrvatin, S., Sun, S., Wilcox, O.F., Yao, H., Lavin-Peter, A.J., Cicconet, M., Assad, E.G., Palmer, M.E., Aronson, S., Banks, A.S., Griffith, E.C. & Greenberg, M.E. (2020) Neurons that regulate mouse torpor. *Nature*, **583**, 115-121.

Klingenberg, M. & Winkler, E. (1985) The reconstituted isolated uncoupling protein is a membrane potential driven H+ translocator. *EMBO J*, **4**, 3087-3092.

Kutschke, M., Grimpo, K., Kastl, A., Schneider, S., Heldmaier, G., Exner, C. & Jastroch, M. (2013) Depression of mitochondrial respiration during daily torpor of the Djungarian hamster, Phodopus sungorus, is specific for liver and correlates with body temperature. *Comp Biochem Physiol A Mol Integr Physiol*, **164**, 584-589.

Leducq, N., Delmas-Beauvieux, M.C., Bourdel-Marchasson, I., Dufour, S., Gallis, J.L., Canioni, P. & Diolez, P. (1998) Mitochondrial permeability transition during hypothermic to normothermic reperfusion in rat liver demonstrated by the protective effect of cyclosporin A. *Biochem J*, **336 (Pt 2)**, 501-506.

Lee, C.C. (2008) Is human hibernation possible? *Annu Rev Med*, **59**, 177-186.

Luppi, M., Hitrec, T., Di Cristoforo, A., Squarcio, F., Stanzani, A., Occhinegro, A., Chiavetta, P., Tupone, D., Zamboni, G., Amici, R. & Cerri, M. (2019) Phosphorylation and Dephosphorylation of Tau Protein During Synthetic Torpor. *Front Neuroanat*, **13**, 57.

Martin, A.W. & Fuhrman, F.A. (1955) The Relationship between Summated Tissue Respiration and Metabolic Rate in the Mouse and Dog. *Physiol. Zool.*, **28**, 18-34.

Martin, S.L., Maniero, G.D., Carey, C. & Hand, S.C. (1999) Reversible depression of oxygen consumption in isolated liver mitochondria during hibernation. *Physiol Biochem Zool*, **72**, 255-264.

Morrison, S.F., Madden, C.J. & Tupone, D. (2014) Central neural regulation of brown adipose tissue thermogenesis and energy expenditure. *Cell Metab*, **19**, 741-756.

Muleme, H.M., Walpole, A.C. & Staples, J.F. (2006) Mitochondrial metabolism in hibernation: metabolic suppression, temperature effects, and substrate preferences. *Physiol Biochem Zool*, **79**, 474-483.

Nath, S. (2016) The thermodynamic efficiency of ATP synthesis in oxidative phosphorylation. *Biophys Chem*, **219**, 69-74.

Paxinos, G. & Watson, C. (2007) *The rat brain in stereotaxic coordinates*. Elsevier San Diego.

Pehowich, D.J. & Wang, L.C.H. (1984) Seasonal changes in mitochondrial succinate dehydrogenase activity in a hibernator,Spermophilus richardsonii. *J. Comp. Physiol. B*, **154**, 495 - 501.

Puspitasari, A., Cerri, M., Takahashi, A., Yoshida, Y., Hanamura, K. & Tinganelli, W. (2021) Hibernation as a Tool for Radiation Protection in Space Exploration. *Life (Basel)*, **11**.

Rolfe, D.F. & Brown, G.C. (1997) Cellular energy utilization and molecular origin of standard metabolic rate in mammals. *Physiol Rev*, **77**, 731-758.

Solaini, G., Baracca, A., Gabellieri, E. & Lenaz, G. (1997) Modification of the mitochondrial F1-ATPase epsilon subunit, enhancement of the ATPase activity of the IF1-F1 complex and IF1-binding dependence of the conformation of the epsilon subunit. *Biochem J*, **327 (Pt 2)**, 443-448.

Solaini, G., Harris, D.A., Lenaz, G., Sgarbi, G. & Baracca, A. (2008) The study of the pathogenic mechanism of mitochondrial diseases provides information on basic bioenergetics. *Biochim Biophys Acta*, **1777**, 941-945.

Staples, J.F. (2014) Metabolic suppression in mammalian hibernation: the role of mitochondria. *J Exp Biol*, **217**, 2032-2036.

Staples, J.F. & Brown, J.C. (2008) Mitochondrial metabolism in hibernation and daily torpor: a review. *J Comp Physiol B*, **178**, 811-827.

Susantitaphong, P., Alfayez, M., Cohen-Bucay, A., Balk, E.M. & Jaber, B.L. (2012) Therapeutic hypothermia and prevention of acute kidney injury: a meta-analysis of randomized controlled trials. *Resuscitation*, **83**, 159-167.

Takahashi, T.M., Sunagawa, G.A., Soya, S., Abe, M., Sakurai, K., Ishikawa, K., Yanagisawa, M., Hama, H., Hasegawa, E., Miyawaki, A., Sakimura, K., Takahashi, M. & Sakurai, T. (2020) A discrete neuronal circuit induces a hibernation-like state in rodents. *Nature*, **583**, 109-114.

Takaki, M., Nakahara, H., Kawatani, Y., Utsumi, K. & Suga, H. (1997) No suppression of respiratory function of mitochondrial isolated from the hearts of anesthetized rats with high-dose pentobarbital sodium. *Jpn J Physiol*, **47**, 87-92.

Tinganelli, W., Hitrec, T., Romani, F., Simoniello, P., Squarcio, F., Stanzani, A., Piscitiello, E., Marchesano, V., Luppi, M., Sioli, M., Helm, A., Compagnone, G., Morganti, A.G., Amici, R., Negrini, M., Zoccoli, A., Durante, M. & Cerri, M. (2019) Hibernation and Radioprotection: Gene Expression in the Liver and Testicle of Rats Irradiated under Synthetic Torpor. *Int J Mol Sci*, **20**.

Tupone, D., Madden, C.J. & Morrison, S.F. (2013) Central activation of the A1 adenosine receptor (A1AR) induces a hypothermic, torpor-like state in the rat. *J Neurosci*, **33**, 14512-14525.

Van Dam, K., Westerhoff, H.V., Krab, K., van der Meer, R. & Arents, J.C. (1980) Relationship between chemiosomotic flows and thermodynamic forces in oxidative phosphorylation. *Biochim Biophys Acta*, **591**, 240-250.

Vicent, M.A., Borre, E.D. & Swoap, S.J. (2017) Central activation of the A1 adenosine receptor in fed mice recapitulates only some of the attributes of daily torpor. *J Comp Physiol B*, **187**, 835-845.

Wang, Z., Zhang, J., Ying, Z. & Heymsfield, S.B. (2012) Organ-Tissue Level Model of Resting Energy Expenditure Across Mammals: New Insights into Kleiber's Law. *ISRN Zoology*, **2012**, 673050.

Watt, I.N., Montgomery, M.G., Runswick, M.J., Leslie, A.G. & Walker, J.E. (2010) Bioenergetic cost of making an adenosine triphosphate molecule in animal mitochondria. *Proc Natl Acad Sci U S A*, **107**, 16823-16827.

Wikstrom, M. & Springett, R. (2020) Thermodynamic efficiency, reversibility, and degree of coupling in energy conservation by the mitochondrial respiratory chain. *Commun Biol*, **3**, 451.

Zaretsky, D.V., Zaretskaia, M.V. & DiMicco, J.A. (2003) Stimulation and blockade of GABA(A) receptors in the raphe pallidus: effects on body temperature, heart rate, and blood pressure in conscious rats. *Am J Physiol Regul Integr Comp Physiol*, **285**, R110-116.

Zhang, Z., Reis, F., He, Y., Park, J.W., DiVittorio, J.R., Sivakumar, N., van Veen, J.E., Maesta-Pereira, S., Shum, M., Nichols, I., Massa, M.G., Anderson, S., Paul, K., Liesa, M., Ajijola, O.A., Xu, Y., Adhikari, A. & Correa, S.M. (2020) Estrogen-sensitive medial preoptic area neurons coordinate torpor in mice. *Nat Commun*, **11**, 6378.

Figure legends

Figure 1. Schematic representation of the experimental protocols: A) Protocol used for the "RAT Muscimol" experiment, in which hypothermia was induced by the microinjection of the GABA-A agonist muscimol in the Raphe Pallidus (RPa); B) Protocol used for the "RAT CHA" experiment, in which hypothermia was induced by the i.c.v. injection of the A1AR agonist N_6-cyclohexyladenosine (CHA); C) Protocol used for the "MOUSE" experiment, in which natural torpor was induced by the acute exposure to Ta 15°C, following a 36-h fasting.

Figure 2. Time course of: i) deep brain temperature in rats after the induction of hypothermia by either A) the microinjection of the GABA-A agonist muscimol in the Raphe Pallidus (RPa) (panel A), or the i.c.v. administration of the A1AR agonist N_6-cyclohexyladenosine (CHA) (panel B); ii) cutaneous temperature in mice after the onset of natural torpor induced by the acute exposure to Ta 15°C, following a 36-h fasting (panel C). Control rats were injected with artificial cerebrospinal fluid (ACSF). All data are expressed as mean ± S.E.M. Filled symbols = natural torpor or drug-induced hypothermia experimental groups. Open symbols = controls. *=$p<0.05$, **=$p<0.01$.

Figure 3. Typical Complex I-driven oxygen consumption traces of mitochondria isolated from liver of rat (A and B) and mouse (C) under different experimental conditions. State 3, maximal phosphorylating rate condition obtained in the presence of saturating ADP concentration, and State 4 mitochondrial respiration (absence of ADP phosphorylation) are shown. The saturating oxygen concentration (100%) is 204.1 μM. Due to technical characteristics of the oxygen electrode, the O_2 concentration at the starting of the assay might differ slightly from 100 %.

Figure 4. Mitochondrial respiratory parameters determined in the liver. Following the induction of hypothermia in rats by either the microinjection of the GABA-A agonist muscimol in the Raphe Pallidus (RPa) (panel A) or the i.c.v. administration of the A1AR agonist N_6-cyclohexyladenosine (CHA) (panel B) the respiratory parameters were evaluated. In mice (Panel C) the onset of natural torpor was induced by both acute exposure to Ta of 15°C and 36-h fasting. Control rats were injected with artificial cerebrospinal fluid (ACSF). OCR, Oxygen Consumption Rate. All data are expressed as mean ± S.E.M. Black bars refer to natural torpor or drug-induced hypothermia experimental groups. White bars indicate controls. *$p<0.05$, **$p<0.01$.

Figure 5. Typical Complex I-driven oxygen consumption traces of mitochondria isolated from rat (A and B) and mouse (C) kidney under different experimental conditions.

Figure 6. Mitochondrial respiratory parameters determined in the kidney. Following the induction of hypothermia in rats by either the microinjection of the GABA-A agonist muscimol in the Raphe Pallidus (RPa) (panel A) or the i.c.v. administration of the A1AR agonist N_6-cyclohexyladenosine (CHA) (panel B) the respiratory parameters were evaluated. In mice (Panel C) the onset of natural torpor was induced by both acute exposure to Ta of 15°C and 36-h fasting. Control rats were injected with artificial cerebrospinal fluid (ACSF). OCR, Oxygen Consumption Rate. All data are expressed as mean ± S.E.M. Black bars refer to natural torpor or drug-induced hypothermia experimental groups. White bars indicate controls. *$p<0.05$, **$p<0.01$.

Figures

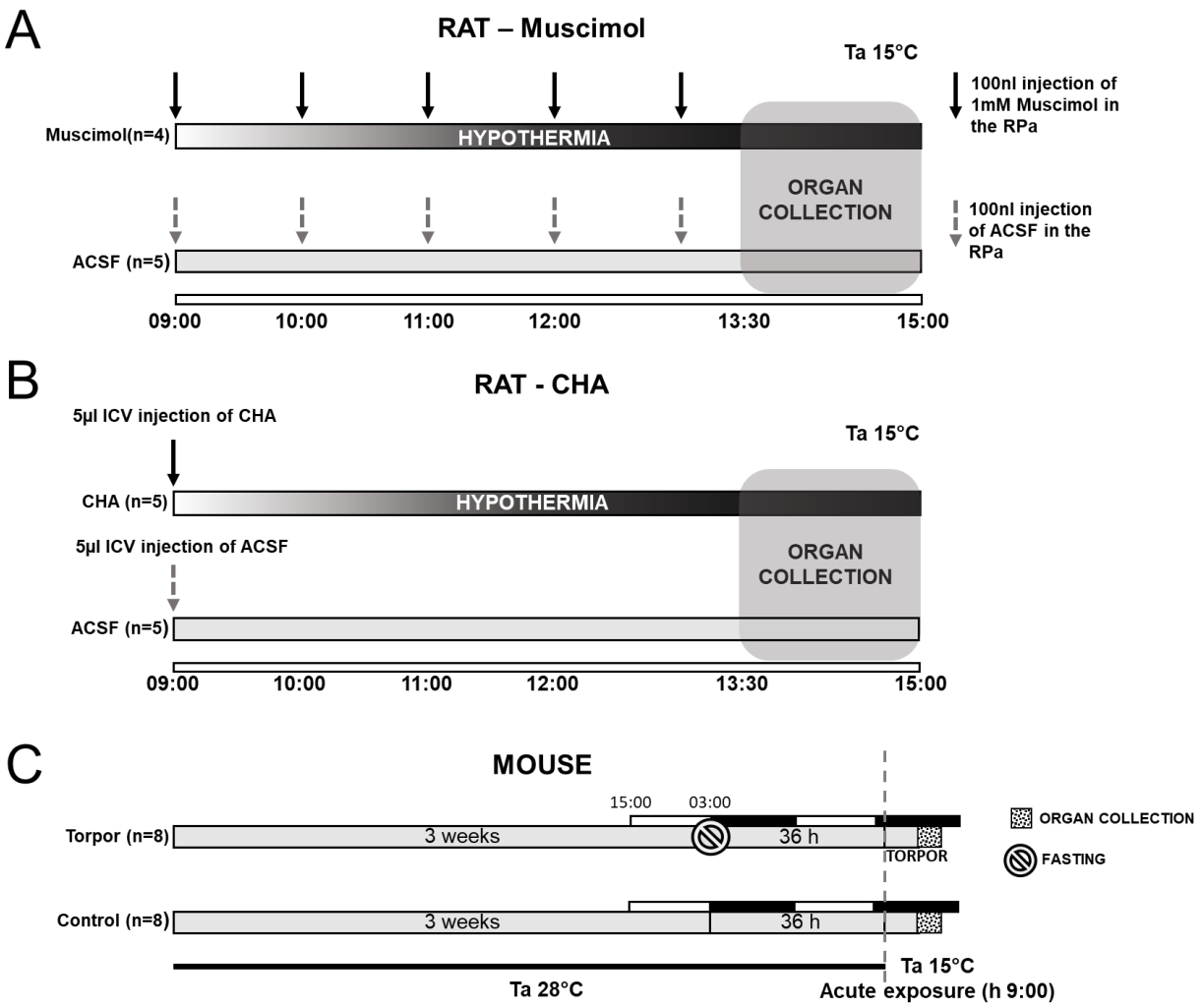
A
RAT – Muscimol
Ta 15°C
100nl injection of 1mM Muscimol in the RPa
Muscimol(n=4)
HYPOTHERMIA
ORGAN COLLECTION
100nl injection of ACSF in the RPa
ACSF (n=5)
09:00
10:00
11:00
12:00
13:30
15:00
B
RAT - CHA
5µl ICV injection of CHA
Ta 15°C
CHA (n=5)
HYPOTHERMIA
5µl ICV injection of ACSF
ORGAN COLLECTION
ACSF (n=5)
09:00
10:00
11:00
12:00
13:30
15:00
C
MOUSE
15:00
03:00
Torpor (n=8)
3 weeks
36 h
TORPOR
ORGAN COLLECTION
FASTING
Control (n=8)
3 weeks
36 h
Ta 15°C
Ta 28°C
Acute exposure (h 9:00)

Figure 1

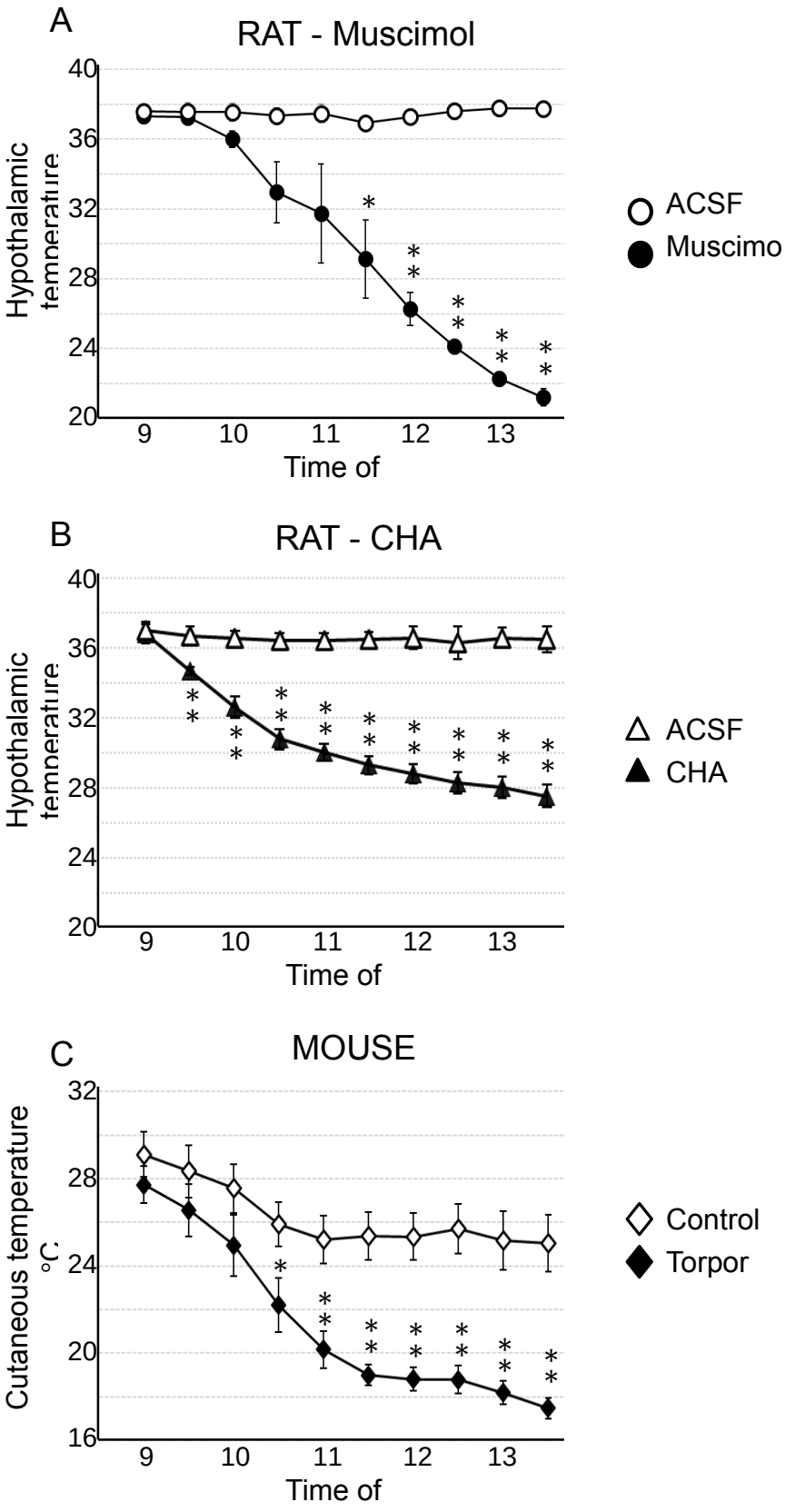
A
RAT - Muscimol
Hypothalamic temperature
40
36
32
28
24
20
9
10
11
12
13
Time of
ACSF
Muscimo
B
RAT - CHA
Hypothalamic temperature
40
36
32
28
24
20
9
10
11
12
13
Time of
ACSF
CHA
C
MOUSE
Cutaneous temperature °C
32
28
24
20
16
9
10
11
12
13
Time of
Control
Torpor

Figure 2.

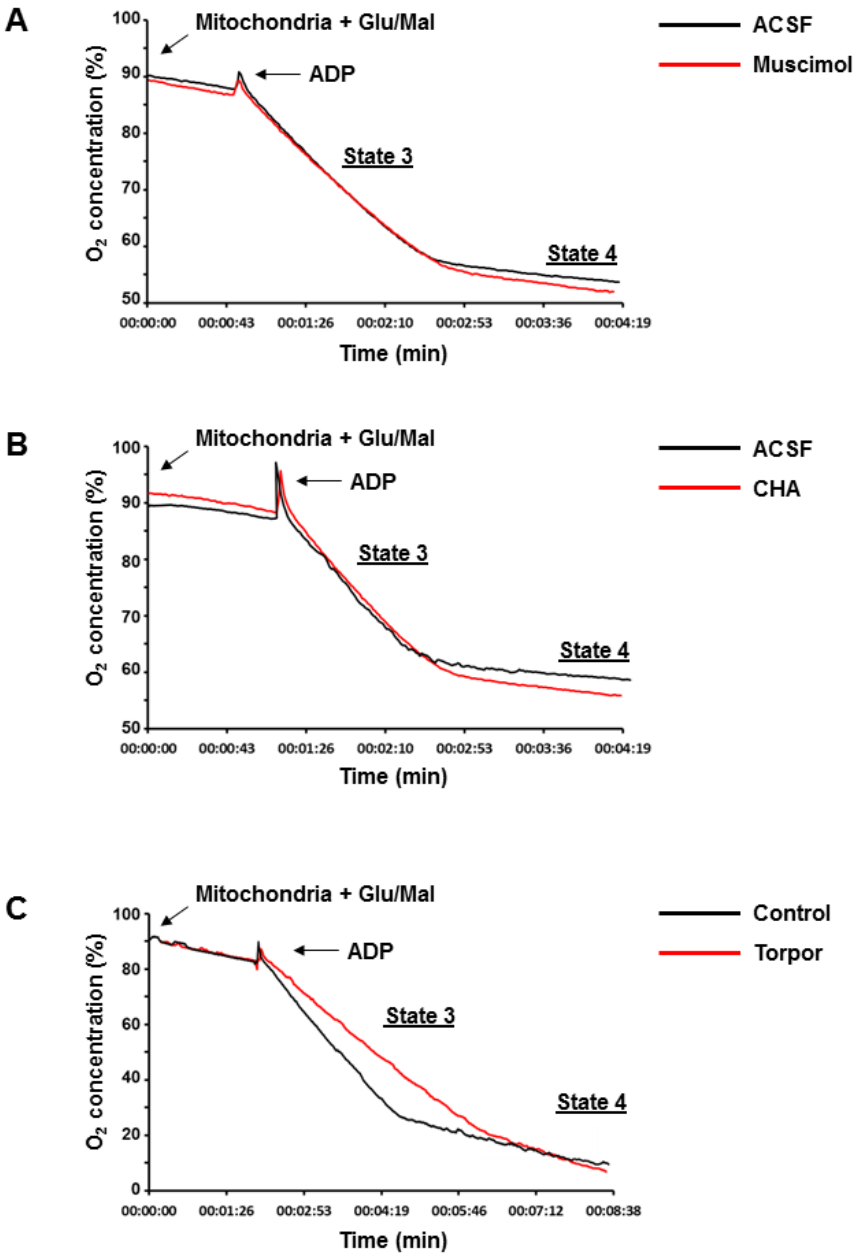
A
Mitochondria + Glu/Mal
ADP
State 3
State 4
ACSF
Muscimol
O2 concentration (%)
Time (min)
B
Mitochondria + Glu/Mal
ADP
State 3
State 4
ACSF
CHA
O2 concentration (%)
Time (min)
C
Mitochondria + Glu/Mal
ADP
State 3
State 4
Control
Torpor
O2 concentration (%)
Time (min)

Figure 3.

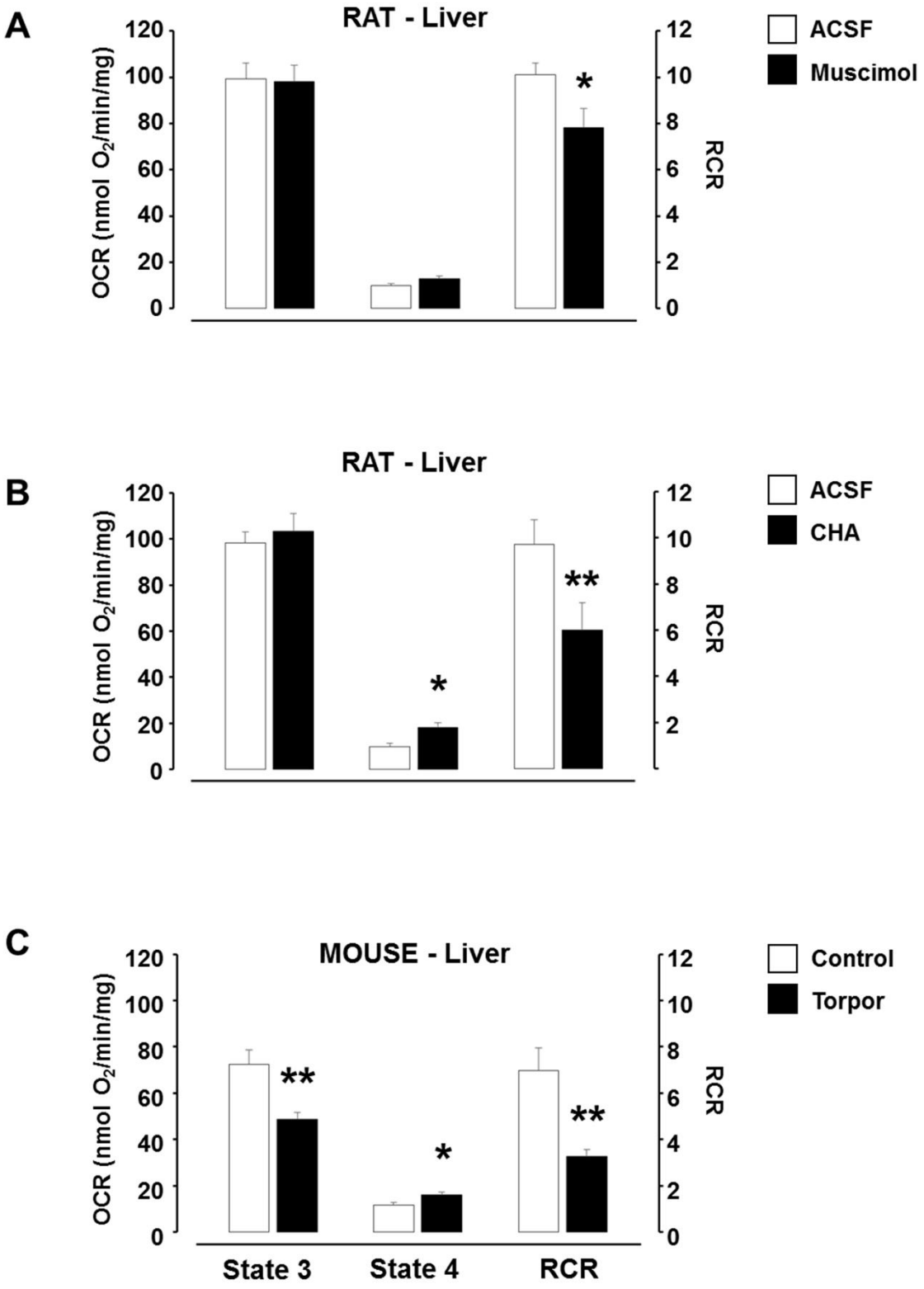
A
RAT - Liver
OCR (nmol O2/min/mg)
RCR
ACSF
Muscimol
*
B
RAT - Liver
OCR (nmol O2/min/mg)
RCR
ACSF
CHA
**
*
C
MOUSE - Liver
OCR (nmol O2/min/mg)
RCR
Control
Torpor
**
*
**
State 3
State 4
RCR

Figure 4.

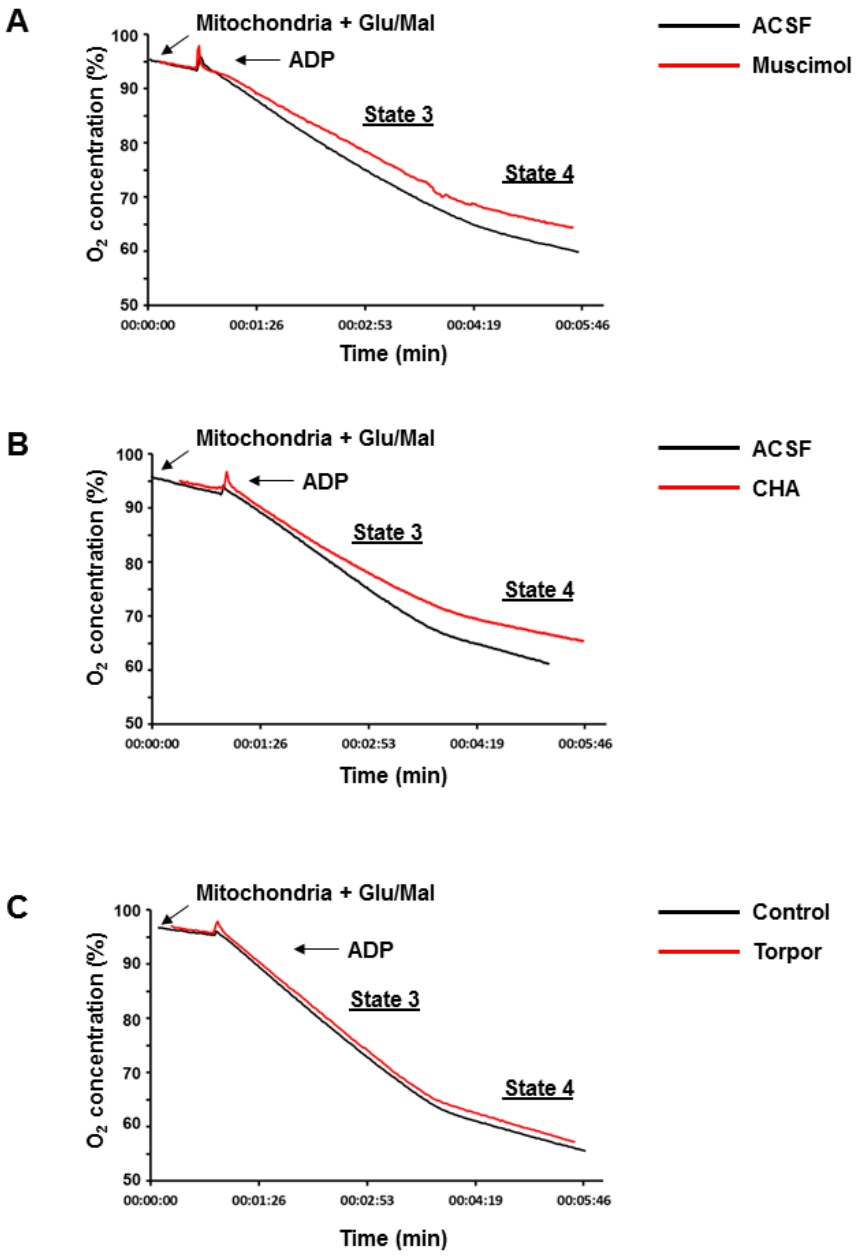
A
Mitochondria + Glu/Mal
ADP
State 3
State 4
ACSF
Muscimol
O2 concentration (%)
100
90
80
70
60
50
00:00:00
00:01:26
00:02:53
00:04:19
00:05:46
Time (min)
B
Mitochondria + Glu/Mal
ADP
State 3
State 4
ACSF
CHA
O2 concentration (%)
Time (min)
C
Mitochondria + Glu/Mal
ADP
State 3
State 4
Control
Torpor
O2 concentration (%)
Time (min)

Figure 5.

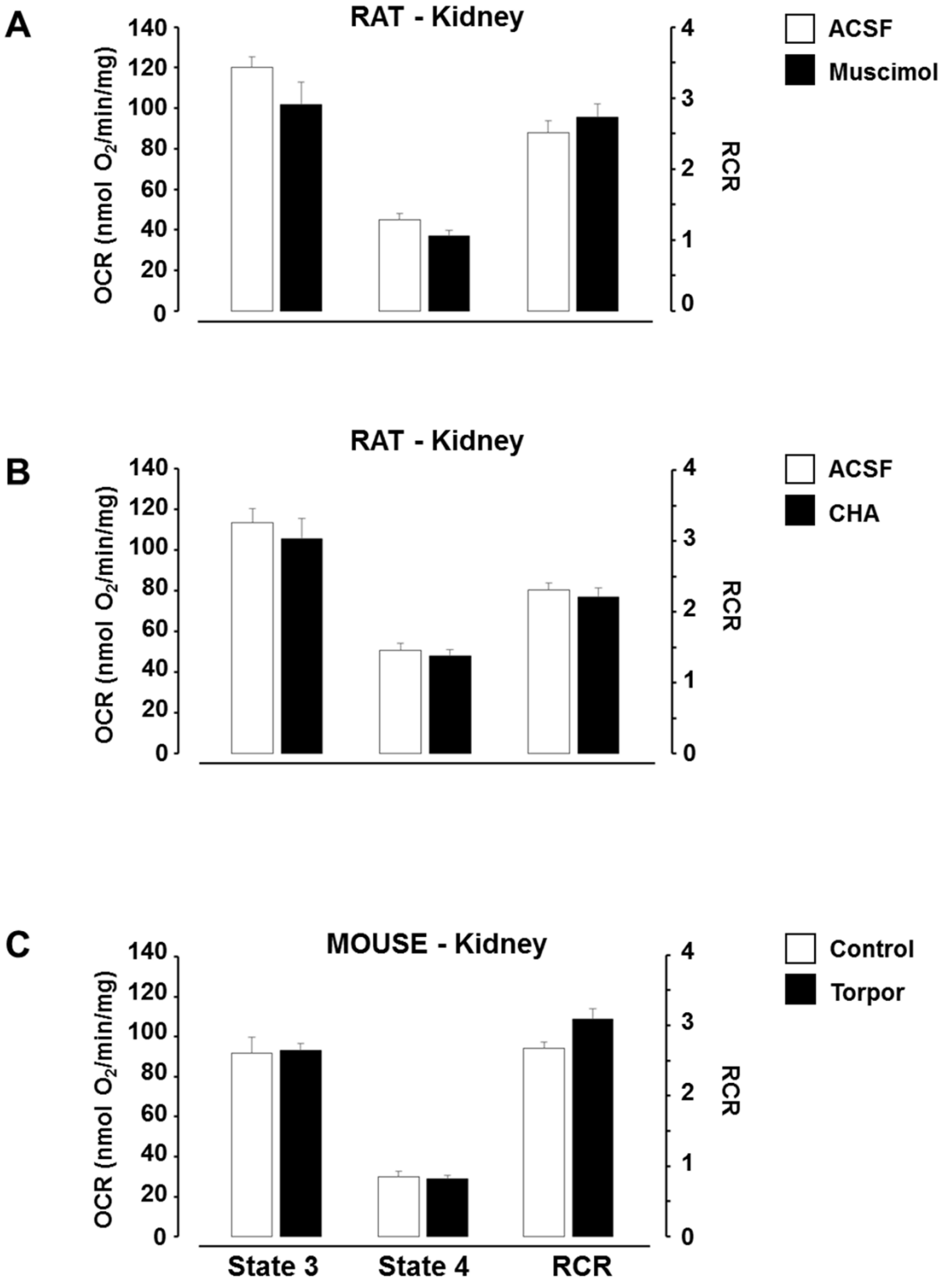

Figure 6 References